PAMELA recent results on galactic proton and helium

Marco Casolino, N. De Simone, V. Formato

INFN and University of Rome Tor Vergata,Via Della Ricerca Scientifica 1, 00133, Rome, Italy

PAMELA is a satellite borne experiment designed to study with great accuracy cosmic rays of galactic, solar, and trapped nature in a wide energy range (protons: 80 MeV-1200 GeV, electrons 50 MeV-600 GeV). Main objective is the study of the antimatter component: antiprotons (80 MeV-190 GeV), positrons (50 MeV-270 GeV) and search for antinuclei (with a precision of the order of 10^{-8}). The experiment, housed on board the Russian Resurs-DK1 satellite, was launched on June, 15th 2006 in a 350×600 km orbit with an inclination of $70°$. In this work we report on the recent results on proton and helium of galactic origin, their solar modulation and the helium isotopic component.

1. Introduction

The scientific program of the Wizard collaboration is devoted to the study of cosmic rays through balloon and satellite-borne devices. Aims of this research involve the precise determination of the antiproton [1] and positron [2] spectra, search of antimatter, measurement of low energy trapped and solar cosmic rays with the NINA-1 [3] and NINA-2 [4] satellite experiments. Other research on board Mir and International Space Station has involved the measurement of the radiation environment, the nuclear abundances and the investigation of the Light Flash [5] phenomenon with the Sileye experiments [6,7]. **PAMELA** is the largest and most complex device built insofar by the collaboration, with the broadest scientific goals. In this work we describe the recent results on proton and helium of galactic origin, their flux modulation due to solar activity and the helium isotope ratio.

2. PAMELA detector

PAMELA (Fig. 1) is constituted by a number of highly redundant detectors capable of measuring charge, rigidity and velocity of particles over a very wide energy range. The instrument is built around a permanent magnet with a silicon microstrip tracker and a scintillator system to provide trigger, charge and time of flight information. A silicon-tungsten calorimeter is used to perform hadron/lepton separation. A shower tail catcher and a neutron detector at the bottom of the apparatus are also employed to improve this separation. An anticounter system rejects off line spurious events produced in the side of the main body of the satellite. Around the detectors are housed the readout electronics, the interfaces with the CPU and all primary and secondary power supplies. All systems (power supply, readout boards etc.) are redundant with the exception of the CPU which is more tolerant to failures. The system is enclosed in a pressurized container located on one side of the Resurs-DK1 satellite. Total weight of **PAMELA** is 470 kg; power consumption is 355 W, geometrical factor is 21.6 cm^2 sr. A more detailed description of the device and the data handling can be found in [8–10]. The satellite was launched on June 15th 2006 in a $70°$ inclination 350×600 km elliptical orbit around the Earth [11] and - at the time of writing - has been working for more than four years.

3. Galactic cosmic rays

Since the discovery of cosmic rays, various mechanisms have been proposed to explain the acceleration of particles to relativistic energies and their subsequent propagation in the Galaxy. It was pointed out long ago (e.g. [12,13]) that supernovae fulfill the power requirement to energize galactic cosmic rays. Subsequently, models were
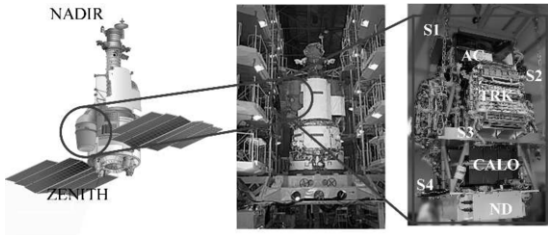
Figure 1. Left: Scheme of the Resurs-DK1 satellite. PAMELA is located in the pressurized container on the left of the picture. In the scheme the pressurized container is in the acquisition configuration. Center: The Resurs-DK1 satellite during integration in Samara. The pressurized container housing PAMELA is in the folded (launch) position. Right: Photo of the PAMELA detector during integration in Tor Vergata with marked the position of the detectors. S1, S2, S3, S4: scintillator planes; AC: top anticoincidence; TRK: tracker core; CALO: Silicon-Tungsten calorimeter; ND: Neutron Detector.

put forward to explain the acceleration of cosmic ray particles as diffusive shock acceleration ("first order Fermi mechanism") produced by supernova (SN) shock waves propagating in the interstellar medium (see [14,15] for a review). This simple SN-only paradigm has been challenged several times in the past with authors introducing several different sources or acceleration models to describe data in the 1 - 10^7 GeV range [16,17].

Evidence for SN shock acceleration of cosmic rays to a maximum energy of $\simeq 3 \times 10^{15}$ eV comes from a number of observations. For example, TeV emission from the young supernova remnant (SNR) RX J1713.7-3946, detected by the H.E.S.S. collaboration [18], has been interpreted as originating from hadronic interactions of cosmic rays with energies above 10^{14} eV in the shell of the SNR (even though leptonic processes cannot be ruled out [19]). X-ray measurements of the same SNR provide evidence that protons and nuclei can be accelerated to energies $\geq 10^{15}$ eV [20]. Recent AGILE observations of diffuse gamma ray emission in the 100 MeV - 1 GeV range from the outer shock region of SNR IC 443 have been explained

in terms of hadronic acceleration [21]. Likewise, Fermi observations of the shell of SNR W44 have been attributed to the decay of π^0s produced during interactions of accelerated hadrons with the interstellar medium [22].

The hypothesis that cosmic rays are accelerated in supernova explosions is further corroborated by observations of other galaxies. In starburst galaxies (SG), the SN rate at the galactic center is much higher than in the Milky Way and the density of cosmic rays deduced from observations of TeV gamma rays is much higher. This has been confirmed by H.E.S.S. which measures gamma rays with energies $\geq$ 220 GeV. At the end of the acceleration phase, particles are injected into the interstellar medium where they propagate, diffusing in the turbulent galactic magnetic fields. Nowadays, this propagation is well described by solving numerically (e.g. the GALPROP simulation code [23]) or analytically (e.g. [24]) the transport equations for the particle diffusion in the Galaxy. One of the most striking features of cosmic ray spectra measured prior to PAMELA observations is that they are apparently featureless. Up to now, the spectra have been described by a single power law for each species, with similar spectral indices ($\gamma \simeq -2.7$) for protons and heavier nuclei, up to energies of $\approx 10^{15}$ eV (the so called 'knee' region) as predicted by the shock diffusion acceleration model and diffusive propagation in the Galaxy. Recent PAMELA measurements of the antiparticle component of the cosmic radiation [2,25,26] have prompted a re-evaluation of possible contributions from additional galactic sources, either of astrophysical (such as pulsars [27]) or exotic (dark matter [28]) origin. A precise determination of the proton and helium fluxes, the most abundant components in cosmic rays, is of crucial importance for the understanding of astrophysical phenomena taking place in the Galaxy, in the galactic neighborhood of the Sun (1-2 kpc radius) and within the solar system. With a detailed knowledge of cosmic ray spectra it will be possible to: a) identify sources and acceleration/propagation mechanisms of cosmic rays; b) estimate the production of secondary particles, such as positrons and antiprotons, in order to disentangle the secondary particle com-
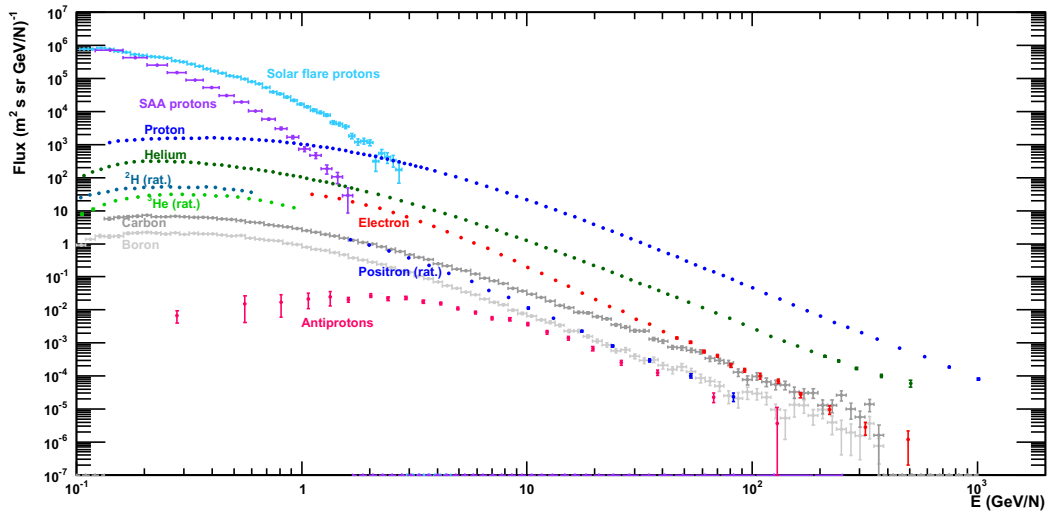
Figure 2. Differential spectrum of particles measured with PAMELA. The most abundant component is due to protons of galactic origin, with solar particles increasing by several orders of magnitude for a short time. Trapped particles in the inner Van Allen belt dominate in some regions of Low Earth Orbit. The antiparticle component of antiprotons and positrons is the least abundant one. Deuterium, He^3 and e^+ fluxes have been calculated from the ratios.

ponent from possible exotic sources; c) estimate the particle flux in the geomagnetic field and in Earth's atmosphere for in-orbit dose estimations and to derive the atmospheric muon and neutrino flux, respectively. In Figure 3 are shown the proton and helium fluxes measured with PAMELA as function of the kinetic energy. Below about 30 GeV, the differences are due to different solar modulation conditions between the various measurements. At $\simeq 200$ GV both spectra show an increase of the flux, hinting probably to an additional source which is injecting particles above this energy.

In Fig. 4 the $^3He/^4He$ ratio as a function of both kinetic energy per nucleon and rigidity is shown. The error bars show the statistical error, and the shaded regions show the systematic uncertainty of the measure. Previous experimental measurements, with lower statistics and affected by additional sources of systematic error like the residual atmosphere present in balloon experiments, are in agreement with PAMELA data. The

curves show the prediction of diffusive reacceleration model and plain diffusion model evaluated with GALPROP [42] (see the caption for further details) for different values of the solar modulation parameter in the spherical force-field approximation [43] (450, 550, and 800 MV). The high statistics collected by PAMELA allows for the first time to discriminate between the standard theoretical models, in particular probing the presence of reacceleration processes in cosmic rays propagation. All measurements have been taken at the minimum activity of Solar cycle 23 so, as expected from models, there is no evident change with time and even at solar maximum condition the model predicts that the difference with respect to solar minimum condition is $\sim 20\%$ at low energy and decreases with increasing rigidity. Although the data are in better agreement with the reacceleration model, a future comparison of D/H ratio will help to better understand the phenomena taking place in galactic propagation.
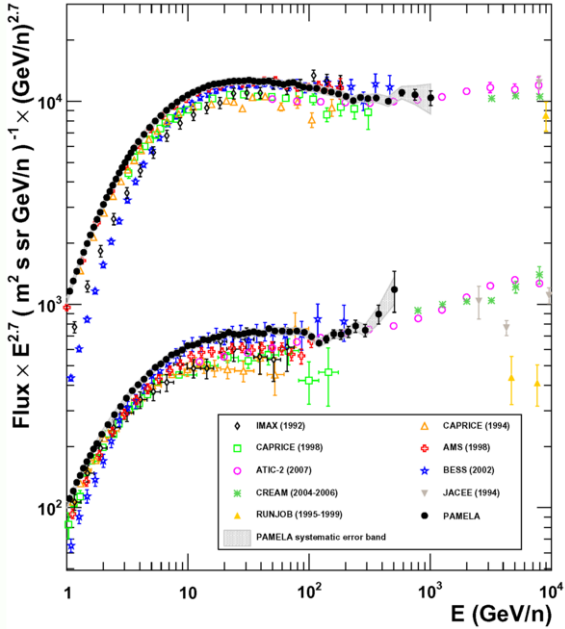
Figure 3. Proton and helium absolute fluxes measured by PAMELA above 1 GeV/n, compared with some previous measurements [29–36]. Error bars are statistical, the shaded area represents the estimated systematic uncertainty. From the plots it is possible to see the different spectral indexes for the two species and a change in the spectral slopes above $\simeq 200$ GeV/n.

4. Galactic cosmic rays and solar modulation

Launch of PAMELA occurred during the XXIII solar minimum; in this phase the magnetic field of the Sun has an approximatively dipolar structure, currently with negative polarity (A<0, with magnetic field lines directed toward the Sun in the northern emisphere). We are currently in an unusually long solar minimum with various predictions on the behavior of the intensity and peaking time of next maximum. In the 2006-2009 period PAMELA has been observing an increase of the flux of galactic cosmic rays at low energy (< 10 GeV) due to solar modulation caused by the decreasing solar activity. A long term measurement of the behaviour of the proton, electron and $Z \geq 2$
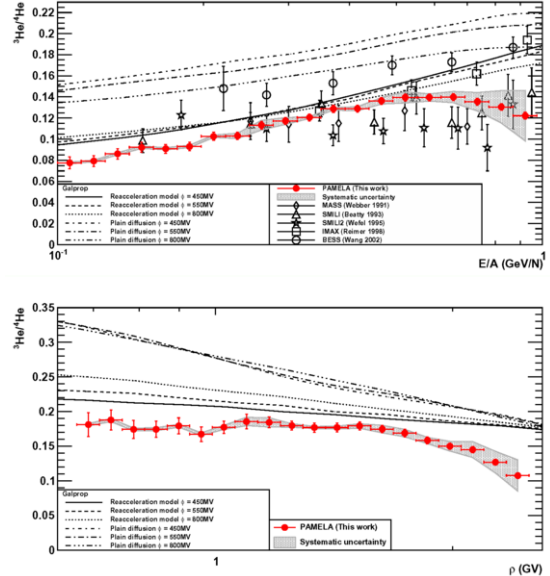
Figure 4. ^{3}He/^{4}He ratio as a function of kinetic energy per nucleon (top) and rigidity (bottom). The error bars show the statistical error, and the shaded regions show the systematic uncertainty of the measure. Previous measurements [37–41] are shown together with theoretical predictions by Strong and Moskalenko. [42].

flux at 1 AU can provide information on propagation phenomena occurring in the heliosphere. The possibility to measure the antiparticle spectra will allow to study also charge dependent solar modulation effects.

In Fig. 5 the proton fluxes measured in various periods of the mission are shown. The effect of decreasing solar activity on the increasing flux of cosmic rays is visible even at solar quiet period, in agreement with the increase of ground neutron monitor fluxes. From the flux $J(E, t)$ it is possible to evaluate the solar modulation parameter $\Phi(t)$. The heliosphere is thus approximated with a spherical potential [43], assuming that particles lose energy independently from the sign of the charge and incoming direction to enter the heliosphere according to the following:

$$J(E, t) = \frac{E^2 - E_0^2}{(E + |Z|e\Phi(t))^2 - E_0^2} J_{is}(E + |Z|e\Phi(t)) \quad (1)$$

More detailed models involve numerical solu-
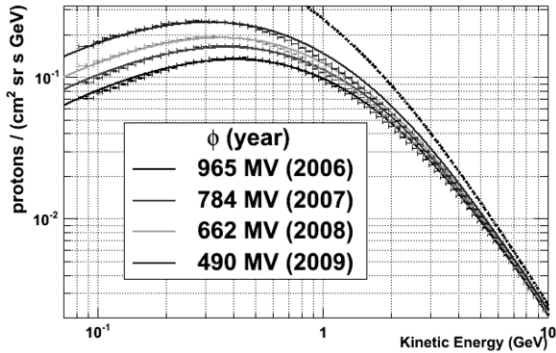
Figure 5. Differential spectrum of protons measured in 2006 (black), 2007 (red), 2008 (green) and 2009 (blue). Below 1 GeV it is possible to see the effect of solar modulation on the flux variation. The dotted black line represent the assumed local interstellar spectrum.

tions of the Parker's transport equation taking also into account drift effects. Eq. 1 can be used to fit PAMELA proton data but a model of LIS J_{is} has to be chosen, since it has never been directly measured. The resulting values of Φ will be strongly dependent on this choice. In this work we will consider the LIS as determined using the GALPROP program with the propagation parameters of the so called "conventional diffusion model" [44]. The minimization of the fit of Eq. 1 is done by using the program MINUIT [45].
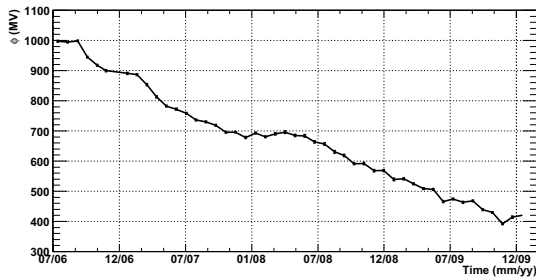
Figure 6. Solar modulation parameter Φ as a function of time, calculated every Carrington rotation from the fit of Eq. 1.

Fig. 6 shows the decrease of the solar modulation parameter from 2006 to 2009 where Φ is calculated every Carrington rotation from the fit of Eq. 1.

REFERENCES

1. O. Adriani, *et al.*, *Physical Review Letters* **102**, 051101 (2009).
2. O. Adriani, *et al.*, *Nature* **458**, 607 (2009).
3. V. Bidoli, *et al.*, *ApJS* **132**, 365 (2001).
4. V. Bidoli, *et al.*, *Journal of Geophysical Research (Space Physics)* **108**, 1211 (2003).
5. M. Casolino, *et al.*, *Nature* **422**, 680 (2003).
6. V. Bidoli, *et al.*, *Journal of Physics G Nuclear Physics* **27**, 2051 (2001).
7. M. Casolino, *et al.*, *Advances in Space Research* **37**, 1691 (2006).
8. P. Picozza, *et al.*, *Astroparticle Physics* **27**, 296 (2007).
9. M. Casolino, *et al.*, *Advances in Space Research* **37**, 1857 (2006).
10. M. Casolino, *et al.*, *Advances in Space Research* **37**, 1884 (2006).
11. M. Casolino, The Pamela collaboration, *ArXiv e-prints* (2009).
12. P. O. Lagage, C. J. Cesarsky, *Astron. Astrophys.* **118**, 223 (1983).
13. V. L. Ginzburg, S. I. Syrovatskii, *The Origin of Cosmic Rays* (1964).
14. A. R. Bell, *Monthly Notices of the Royal Astronomical Society* **182**, 147 (1978).
15. M. A. Malkov, L. O'C Drury, *Reports on Progress in Physics* **64**, 429 (2001).
16. A. R. Bell, S. G. Lucek, *Monthly Notices of the Royal Astronomical Society* **283**, 1083 (1996).
17. V. I. Zatsepin, N. V. Sokolskaya, *Astron. Astrophys.* **458**, 1 (2006).
18. F. Aharonian, *et al.*, *Astron. Astrophys.* **464**, 235 (2007).
19. D. C. Ellison, D. J. Patnaude, P. Slane, J. Raymond, *Astrophysical Journal* **712**, 287 (2010).
20. Y. Uchiyama, F. A. Aharonian, T. Tanaka, T. Takahashi, Y. Maeda, *Nature* **449**, 576 (2007).
21. M. Tavani, *et al.*, *ApJL* **710**, L151 (2010).
22. A. A. Abdo, *et al.*, *Science* **327**, 1103 (2010).
23. A. W. Strong, I. V. Moskalenko, *Astrophysical Journal* **509**, 212 (1998).
24. F. Donato, *et al.*, *Astrophysical Journal* **563**, 172 (2001).

25. O. Adriani, *et al.*, *Physical Review Letters* **102**, 051101 (2009).

26. O. Adriani, *et al.*, *Phys. Rev. Lett.* **105**, 121101 (2010).

27. C. Grimani, *Classical and Quantum Gravity* **26**, 235009 (2009).

28. G. Kane, R. Lu, S. Watson, *Physics Letters B* **681**, 151 (2009).

29. W. Menn, M. Hof, O. Reimer, M. Simon, *et al.*, *Astrophysical Journal* **533**, 281 (2000).

30. M. Boezio, P. Carlson, T. Francke, N. Weber, *et al.*, *Astrophysical Journal* **518**, 457 (1999).

31. M. Boezio, V. Bonvicini, P. Schiavon, A. Vacchi, *et al.*, *Astroparticle Physics* **19**, 583 (2003).

32. J. Alcaraz, B. Alpat, G. Ambrosi, H. Anderhub, *et al.*, *Physics Letters B* **490**, 27 (2000).

33. J. P. Wefel, J. J. H. Adams, H. S. Ahn, et al., *International Cosmic Ray Conference* (2008), vol. 2 of *International Cosmic Ray Conference*, pp. 31–34.

34. T. Sanuki, H. Matsumoto, M. Nozaki, K. Abe, *et al.*, *Advances in Space Research* **27**, 761 (2001).

35. H. S. Ahn, *et al.*, *ApJL* **714**, L89 (2010).

36. S. Haino, *et al.*, *Physics Letters B* **594**, 35 (2004).

37. J. Z. Wang, E. S. Seo, *et al.*, *Astrophysical Journal* **564**, 244 (2002).

38. G. A. de Nolfo, *et al.*, *Acceleration and Transport of Energetic Particles Observed in the Heliosphere*, R. A. Mewaldt, J. R. Jokipii, M. A. Lee, E. Möbius, & T. H. Zurbuchen , ed. (2000), vol. 528 of *American Institute of Physics Conference Series*, pp. 425–428.

39. O. Reimer, *et al.*, *Astrophysical Journal* **496**, 490 (1998).

40. W. R. Webber, R. L. Golden, S. J. Stochaj, J. F. Ormes, R. E. Strittmatter, *Astrophysical Journal* **380**, 230 (1991).

41. J. J. Beatty, *et al.*, *Astrophysical Journal* **413**, 268 (1993).

42. A. W. Strong, *et al.*, *ArXiv e-prints* (2009).

43. L. J. Gleeson, W. I. Axford, *Astrophysical Journal* **154**, 1011 (1968).

44. A. E. Vladimirov, *et al.*, *1008.3642* (2010).

45. F. James, M. Roos, *Computer Physics Communications* **10**, 343 (1975).